demonstrated by localizing artificially produced sinks and sources in the cerebellar and cerebral cortices *(68, 192, 218)*.

Experimentally, the profiles of field potentials are obtained by measurements at discrete equidistant locations, and the second spatial derivative is calculated according to a finite difference formula *(66)*. Most commonly, the second spatial derivative is approximated by

$$\frac{\partial^2 \phi}{\partial z^2} \approx \frac{\phi(z + n \cdot \Delta z) - 2\phi(z) + \phi(z - n \cdot Az)}{(n \cdot \Delta z)^2} \qquad (8)$$

where Az is the distance between adjacent recording sites and $n \cdot Az$ is the differentiation grid (usually $n = 1$ or 2). The optimal choice of the differentiation grid depends on the anatomical order of the structure and can be judged from the shape of the potential profile, i.e., the dominant spatial frequency components of the potential *(66, 196)*.

Because total inward and outward membrane currents are equal in amplitude in the physiological situations considered here (see sect. II*C*), monopoles (i.e., imbalanced sinks or sources) can be excluded as possible generators of field potentials. Two types of generators may occur in principle (for details see sect. II*C*). *1)* Sink/source dipoles (or sheets of dipoles) generate a potential field that is positive in the region of the source, negative in the region of the sink, and zero on the equidistant plane between. Beyond the CSD distribution this potential decays only slowly. The limit values for this decay are $\phi \propto 1/z^2$ for one dipole and ϕ = constant (!) for an infinitely extended sheet. This potential field outside the CSD distribution is termed *far field (178)*. ***2)*** Symmetrical arrangements, like a source/sink/source distribution, generate a *closedfield* (178), which is large at the location of the central part of the CSD and decays to zero toward the borders of the CSD This type of potential does not reverse in sign and does not have a far-field component.

In general, the reverse of the CSD analysis is not possible; i.e., field potentials cannot be calculated from CSDs. The CSD analysis reveals the local causes of the field potentials and thereby eliminates far-field contributions. The knowledge of these far fields would be necessary, however, to reconstruct the field potentials from the CSDs.

B. *Experimental CSD Studies*

The CSD method has been applied for analysis of electrically evoked potentials *(3, 28, 61, 64–68, 101, 102, 118, 122,* 140a, *141, 161,* 186a, *195–200, 217, 220, 232, 272, 277, 295, 306, 312, 313,* 317), adequately evoked potentials *(23, 65, 67, 103, 104, 112, 143, 183, 193, 194, 208, 211, 214, 251, 278,* 314), and pathological events *(116, 231, 235, 251, 268, 306)*. It has been used to study ensemble activities in the spinal cord *(118,* 232), the medulla oblongata (141), a thalamic nucleus *(195, 196,* 199), tectal structures *(28, 64, 65, 67,* 186a, *208,*

295, 312, 313), the hippocampal formation (3, 102, 161, 272, 317), the cerebellum *(66, 68, 217,* 220), the prepyriform cortex (101), the neocortex *(61, 112, 116,* 122, 140a, *143, 183, 192, 194, 197–200, 208, 211, 231, 235, 251, 252, 268, 277, 278, 306,* 314), the retina *(103, 104,* 214), and the acoustic neuropil of an insect *(23)*.

The analyses were performed in various degrees of complexity. In several studies the one-dimensional approximation was applied at discrete times to yield the CSD distribution related to a certain potential peak *(3, 28, 61,* 101–*104, 122, 214, 235, 268, 312)*. In most applications, one-dimensional CSD profiles as continuous functions of time were evaluated *(64, 66–68,* 140a, *143, 183,* 186a, *193–200, 208, 211, 231, 251, 252, 272, 277, 278, 295, 306, 313,* 314). In four studies, including the two pioneering works, two-dimensional CSD distributions were calculated *(112, 118, 141, 232)*. The conductivity gradient was measured and taken into account in only five of the above-mentioned applications *(101, 103, 104, 214, 313)*. In three further studies it was measured and found to be negligible *(23, 66, 192)*. Three-dimensional CSDs have been derived from focally evoked potentials by Freeman (65), in a study of regeneration in the toad optic tectum, and by Hoeltzell and Dykes (112), in a recent study of cat somatosensory cortex.

Technically the most elaborate CSD analyses were carried out by Nicholson and Llinás (220), by Nicholson et al. (217), and by Breckow et al. *(23)*. Using clusters of seven microelectrodes fixed together so the tips were arranged equidistant in a three-dimensional grid, they performed real-time, three-dimensional CSD analyses. Nicholson et al. *(217)* even combined this method with the determination of the extracellular [K^+] by using an ion-selective electrode as the central pole. The experimental difficulties in building these elaborate multielectrodes, the expensive electronics for the on-line signal processing, and the increase in tissue damage and distortion due to the complex electrode arrays, however, will probably prevent this type of application from becoming a common tool.

Simultaneous recordings of one-dimensional potential profiles, on the other hand, have been performed in several recent CSD studies *(231, 251, 252, 314)*. Either thin-film metal electrodes *(150, 234, 240)* or multiarrays with equidistant tips constructed from isolated wires *(134, 183, 211)* or from micropipettes *(194)* were used. This type of simultaneous recording with a multielectrode has great advantages. It saves time and hence permits the recording and comparison of many different types of potentials within a period of time, during which the state of the animal as well as the positions of the electrodes in the tissue can be assumed constant *(194)*. It can be applied to record field potentials in freely behaving animals *(134, 143, 177, 183, 201)*. Furthermore, it gives access to unique events. Tissue damage and distortion are also a central problem with the available one-dimensional arrays, however.

A few studies, where the current flow density was extracted from the potential profiles by applying *Equation* 4 instead of *Equation* 5, are closely related to CSD analyses (e.g., refs. *152–154, 305, 306)*. With this type of

analysis, far fields are also eliminated, but the advantage of localization is utilized only partially. Because the extracellular current flow is secondary to the physiologically most relevant sinks and sources, this method does not have any advantage over the CSD method.

C. Interpretation of CSDs

The ambiguity of field potentials and CSDs with respect to the neuronal activities that cause them can only be overcome with additional information (see Fig. 1). The core-conductor theory supplies the relation between membrane currents and neuronal activities. Anatomical and single-unit data from the specific ensemble under investigation can help track down the summation of these currents from individual elements to the macroscopic sinks and sources (***Eq.*** 1). Furthermore, direct experimental manipulations, like repetitive stimulation or application of pharmacological agents, may give the cues to differentiate the types of the contributing neuronal activities. The basic arguments along these lines are summarized in this section (see also ref. 172).

1. Implications of core-conductor theory

The theoretical basis for the relation between membrane currents and neuronal activities of individual elements is well established in the core-conductor theory (110, 246)

a) Activation of axons and axon terminals. Activations of axons cause triphasic membrane currents, inwardly directed at the central site of activation and outwardly directed in front of and behind this zone (178). Due to the rather standardized duration of APs of ~1 ms, the spatial extent of this triphasic membrane current along the axon is proportional to the conduction velocity of the fiber. A conduction velocity of 20 m/s, for example, implies that the instantaneous membrane current is distributed over 20 mm! In the end-arborizations of an axon, the conduction velocity of the AP is markedly reduced, because these branches are nonmyelinated and smaller in diameter (57, 84). Generally it is assumed that the active spike does not invade the presynaptic terminals in the central nervous system (CNS) (97); they are depolarized by the capacitive outward current that flows in front of the AP.

b) *Synaptic activation.* During excitatory synaptic activation, active ionic current flows into the cell at the site of the synapse, and passive (capacitive and ohmic) current of equal amplitude leaves the cell at proximal and more-distant membrane sites (49). Both of these membrane currents are purely monophasic. The spatial distribution of the passive outward current over the cell membrane is determined by the length and the time constant of the

cell membrane and by the time function of the active current (246). It decays exponentially, and its time function dissipates with the distance from the synaptic site. Quantitative estimates were obtained by model calculations: within 0.5–1 length constant, the amplitude of the passive outward current is reduced to 10–30%, its time function is dissipated by a factor of ~2, and the amplitude peak is delayed by ~0.5–2 ms (9, 123, 125, 173, 244). [Length constants in the range of 0.5–1 times the length of dendrites (124, 131, 212) and time constants in the range of 4–24 ms (124,131,182) have been reported.]

The excitatory postsynaptic potential (EPSP) is caused by the charging of the membrane capacitors by the capacitive outward currents. Therefore the amplitude of this current at any location is proportional to the time derivative, i.e., to the slope of the local PSP (8, 244). The return of the intracellular potential from the PSP peak to equilibrium essentially results from the discharging of the membrane capacitors via the local membrane resistors; therefore, no net membrane current flows during this decay phase. During hyperpolarizing inhibitory synaptic activation, the directions of the active and passive currents and of the PSP are reversed; otherwise, in principle, the situation is identical.

However, the locations of the two types of synapses on the neurons commonly differ. Most inhibitory synapses are located at or very proximal to the somata; the excitatory synapses spare the somatic membranes and occupy proximal and distant dendritic sites (31, 32, 59, 93, 236, 242, 254, 256, 285,296,301). The dendritic location of the excitatory synapses suggests that the amplitudes and time functions of the active synaptic inward currents at the dendritic sites cannot be judged from the somatically recorded EPSPs, which are due to the small fraction of the total capacitive current that leaves the cell at the soma membrane. The active inward currents at the dendritic synaptic sites are more coherent and are, on the average, 5–20 times larger than a direct estimate from the slopes of the somatic EPSPs suggest (9, 125, 173, 244).

The strategically optimal location of the somatic inhibitory synapses has different implications. According to geometrical considerations, a large portion of the capacitive current leaves the cell directly through the soma membrane, thereby causing the inhibitory PSP (IPSP). Therefore the time course and amplitude of the active outward current at the synaptic site are well reflected by the slope of the IPSP. The net somatic membrane current results from the difference between the active ionic outward current and the somatic (capacitive and ohmic) inward current. This net somatic outward current is the counterpart of the dendritic membrane currents that flow during this inhibitory synaptic activation. In the nomenclature used by Rall (244), the current flowing into the dendrites is the loss current from the soma compartment. A quantitative estimate of this loss current can be obtained from the phase-frequency diagrams, calculated by Lux (181), for different values of the ratio of dendritic input conductance (ρ) (245). Assuming $\rho = 3$

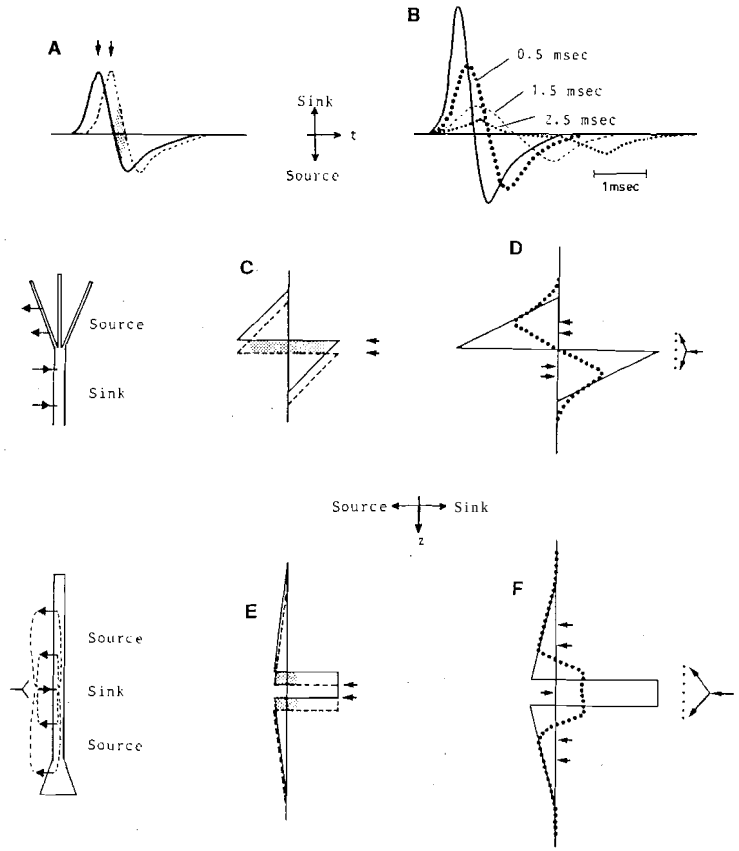

FIG. 2. Schematic illustration of cancelling effects of membrane currents in extracellular space due to temporal and spatial scatter of events. *A:* each *curve* represents time function of net somatic membrane current that flows during generation of soma action potential (AP). Amount of membrane current cancelled in extracellular space due to latency difference of 0.25 ms between the 2 APs is indicated by shaded area. [Curve adapted from Fig. 3a of Terzuolo and Araki (303).] *B*: solid *line* represents time function of current source density (CSD) at soma level of cell ensemble, caused by coherently evoked APs (identical to time function in A). Change of this CSD time function on temporal dissipation of APs is illustrated for scatter of 0.5 ms (*large* dots), 1.5 ms (dashes), and 2.5 ms (small dots). At scatter of 2.5 ms, a CSD-free zone appears between sink and source. *C*: each curve represents spatial distribution of CSD (at some time) along group of accurately aligned activated fiber terminals, as indicated in inset on *left*. (Exponential decays have been approxiniated by linear decays.) Because of steep transition between sink and source, small differences in depth have large cancelling effects (shaded area). *D*: CSD caused by activation of accurately aligned fiber terminals (solid *curve*) becomes smaller in amplitude and smoothed at sink/source transition zone, if terminals scatter in depth (dotted *curve*). Distance between equivalent planes (arrows) of sink and source is enlarged due to scatter. *E*: each curve represents spatial distribution of CSD (at some time) along a group of accurately aligned cells, caused by excitatory synaptic activation, as indicated in inset on *left*. Due to scatter in depth of elements, cancelling occurs at sink/source transition zones (shaded areas). *F*: CSD caused by excitatory synaptic activation (or by first phase of APs) of accurately aligned neurons (solid curve) becomes smaller in amplitude and smoothed at sink/source transition zones, if elements scatter in depth (dotted curve). Distances between equivalent planes (arrows) of sink and sources become larger.

(131, 212), the dendritic loss current is 75% of the active somatic current in the steady-state condition; at active current frequencies of 10, and 50 Hz and 1 kHz, this portion is reduced to 56, 47, and 11%, respectively.

c) Somatic and dendritic APs. During the generation of APs in nerve cells, as in fibers, the current flow is triphasic. At the same membrane location, the passive depolarizing outward current is first followed by inward current and then by outward current; the latter two are the net results of active sodium and potassium currents and a local capacitive current (110). In most cell types the AP is generated in and restricted to the cell soma (e.g., ref. 174).

In the hippocampal pyramidal cells (323), the cerebellar Purkinje cells (174, 219), and immature neocortical cells (243), however, specific types of APs may already be generated in the apical dendrite and may propagate actively down to the soma. These dendritic APs have much slower time courses (3–10 ms in duration) than the usual somatic or fiber APs; their conduction velocity is —0.2 m/s (219). The spatial distribution of membrane currents during the propagation of an AP along a dendrite is similar to that occurring during the propagation of a fiber AP. Capacitive outward current flows in front, and inward and outward currents follow. Probably due to the different types of membrane mechanisms involved here (42, 175), the spatial extent of these membrane currents along the dendrite is smaller (219).

The spatial and temporal distribution of passive as well as active membrane currents during the usual type of somatic AP is rather complicated. The active current can be assumed to be restricted to the soma membrane. The dominant frequency component of this active biphasic current is —1 kHz. Therefore, only 11% of this current is loss current that flows through the dendrites (see above); 89% of it is compensated at the soma membrane, essentially by capacitive current. Because the loss current is identical to the net somatic membrane current, its time course can be estimated from the extracellular potential generated at the soma membrane during the AP (303). A typical example of such a time function is shown in Figure 2*A*. It is biphasic, and its dominant frequency component is —1 kHz. Due to this high temporal frequency, the amplitudes of the passive dendritic membrane currents decay much more steeply with the distance from the soma than those

flowing during the slower inhibitory events (123). This implies that most of the passive current flows proximal to the active current; therefore the corresponding extracellular current loops are confined to the close vicinity of the soma. This is reflected by the empirical fact that the amplitudes of extracellularly recorded APs decay rapidly on retraction of the electrode from the soma (19, 206, 303).

d) Glial cells. The contribution of glial cells to extracellular potentials has been dealt with in several reviews (e.g., refs. 30, 52, 226, 241). The neuroglia appears to be the main cause of slow potentials with frequencies < 1 Hz. In the CNS, significant contributions to faster events can be ruled out according to intracellular data from the cat cortex: the electrically evoked or spontaneous potential changes in these glial cells occur much later and are slower and smaller by a factor of 10 than corresponding PSPs in neurons (95, 96, 249, 250). This implies that the membrane currents of neuroglia are smaller by a factor of 100 and are negligible in comparison with membrane currents from neuronal activities.

In the retina the situation appears to be different. Here the Miiller cells are the only elongated processes, which are oriented perpendicularly to the neuronal and plexiform layers. These glial cells have peculiar conductance properties (214a). Their intracellular potentials correspond well with the b-wave of the electroretinogram, which has a rise time of —200 ms (191). It has therefore been suggested on the basis of a CSD study that the b-wave is caused by K+-currentflow into the Müller cells within the plexiform layers and corresponding outflow at the extreme distal end of the retina (214, 215).

2. *Summation of membrane currents to macroscopic sinks and sources*

To understand the transition from the microlevel of the membrane currents to the macrolevel of the sinks and sources (*Eq.* l), each type of mass activation is considered in an idealized arrangement, then the realistic deviations from this model are outlined.

The idealized arrangement consists of identical elements that are precisely aligned in a two-dimensional sheet; one type of activation is assumed to occur identically and synchronously in all elements In these cases the extracellular volume average of the membrane currents (Eq. 1) can be concluded directly from the individual membrane currents, and the simplest possible CSD distributions result. Because these are homogeneous in the two directions parallel-to the sheet, only the direction perpendicular to the sheet is of concern.

a) Activation of axons and axon terminals. Activation of fibers results in a source/sink/source distribution. This source/sink/source sequence passes through the sheet at the conduction velocity of the fibers. Even for the slowest types of fibers, it extends over 1–2 mm. This implies that the amplitudes of the sink and the two sources are low, compared with more localized events Furthermore, this dissipated CSD distribution is not resolvable in the usual type of CSD applications designed to study a cortex or a nucleus and optimized to resolve events that extend over —50–300 μm (Eq. *8).*

In contrast to the activation of fibers of passage, the activation of terminal arborizations results in a localized sink/source distribution (196, 197). The sink probably results from the last active inward current, and the source in front of it is due to the leading capacitive outward current. This interpretation agrees with the shapes of potentials in the vicinity of cut nerve endings, as described by Lorente de Nó (178). However, because the main components of the afferent activation — the preceding dissipated sinks and sources — are not resolved, this interpretation must remain tentative.

A slight scatter in depth of the terminals leads to a corresponding expansion of the sink and source depth regions. At the external borders, the amplitudes of the sink and source decay according to this scatter. At the central sink/source transition zone, however, nearly total cancellation of opposite membrane currents from nonaligned elements occurs in this situation (Fig. 2*C*). Due to this central cancellation, the distance between the equivalent planes of the resulting sink and source is increased (Fig. 2*D*). Temporal dissipation of the afferent impulses leads to a prolongation and a proportional amplitude reduction of the CSD. This temporal scatter does not cause any cancellation, because the time course of the CSD is monophasic. Examples of this type of activation are the primary afferent activities of the neocortex (197) and of the lateral geniculate nucleus (LGN) (196).

If the fibers (e.g., the cerebellar parallel fibers, the primary afferents of the optic tectum) enter a nucleus tangentially and terminate throughout this layer, the terminals are evenly scattered. In this situation the membrane currents of the terminal regions cancel totally. Therefore, the sink recorded in experiments in such layers of terminals (65, 67, 313) must be due to excess inflow of current into the fibers that terminate at the far end; i.e., in this situation, more of the central sink of the dissipated source/sink/source distribution reaches the nucleus; the counterpart of the resulting excess sink, the final source, does not enter the nucleus.

b) Synaptic activation. Synchronized excitatory (inhibitory) synaptic activation of a sheet of neurons creates a sink (source) at the depth of the synapses and creates sources (sinks) above and below the synapses. Because these sources (sinks) do not extend beyond the neurons, synaptic activation at the far upper or lower ends of the neurons creates a dipolar sink/source distribution only. Because the amplitudes of the passive capacitive currents decay exponentially with the distance from the synápses, the amplitudes of the sources (sinks) decay exponentially with the distance from that synapse level as well. The time functions of these sources (sinks) are more coherent than the time function of the central sink (source) and peak slightly earlier, close to the synaptic level; with distance, they progressively dissipate and peak later. Obliquely arranged dendrites imply a compression of the source (sink) distribution and thereby a reduction of the distance of the equivalent

source (sink) plane from the synaptic plane, but no quantitative loss. The only exception is the horizontal dendrites within the synaptic plane; the source, due to their passive currents, subtracts from the sink.

The effects of scatter of the synaptic activations in depth or time are very similar to those described above for terminal arborizations. Because of the scatter in depth, cancellation occurs at the sink/source transition zones (Fig. 2*E*), thereby smoothing the steep sink/source gradients and increasing the equivalent plane distances (Fig. 2*F*). The spatial expansion at the outer borders of the CSD and the temporal dissipation cause proportional amplitude reductions but no cancellations.

c) Somatic and dendritic *APs.* Synchronous generation of APs in the somata of accurately aligned cells creates a sink, succeeded by a source, at the depth of the somata (see Fig. 2*A*), and a source, then sink, above and below the somata. The amplitudes of the distributions of source followed by sink decay steeply with the distance from the soma region. Obliquely or horizontally oriented dendrites have the same implications here as they do for the passive sources (sinks) during synaptic activations.

Qualitatively, scatter of the somata in depth has the same effect as scatter of synapses, with cancellations at the sink/source transition zones and dissipation of the CSD distribution (see Fig. 2*E*, **F**). Quantitatively, however, this effect is more severe here, because the distances of the equivalent sink and source planes are much smaller (123); i.e., a small amount of scatter in depth of AP-generating somata is equivalent to a much larger scatter of synapses, with respect to the cancelling effect. In contrast to the situation during terminal or synaptic activations, temporal scatter of the APs also causes cancellations, which are due to the biphasic nature of the CSD time function (see Fig. 2*A*). The change in the time function and the amplitude reduction of the CSD due to temporal scatter of the APs is illustrated in Figure 2B. Because of the smooth transition between the sink and the source, the effect of cancelling is rather small for small scatters (see Fig. 2A). It steadily increases up to a scatter of —1.5 ms. From then on, the sink and the source (and their corresponding counterparts above and below) do not dissipate any more. Further scattering leads to a further amplitude reduction and an increasing CSD-free zone between (see Fig. 2*B*). Now all the membrane currents from the successive APs cancel totally; only the first phase of the earliest APs and the last phase of the very last APs remain imbalanced.

The dendritic APs in the apical dendrites of Purkinje cells and hippocampal pyramidal cells cause a source/sink/source distribution, which moves down to the soma level at a velocity of —0.2 m/s. Its instantaneous extent over depth is —300 μm (219). Its triphasic time function — according to the slow time course of the dendritic APs — has a duration of at least 3 ms. The smooth transitions between the sink and the sources, in space as well as in time, imply that small scatter in latency (and the concomitant spatial scatter) have only slight cancelling effects (see Fig. 2*A*). In comparison to the soma APs (see Fig. 2*B*), the time range of scatter may be at least twice as long to cause equivalent effects.

3. Quantitative *comparison of AP- and* PSP-related CSDs *and* experimental *confirmations*

a) Theoretical *estimate.* By combining the considerations of the two preceding sections, a quantitative estimate of the CSD contributions from APs and PSPs can be made. Such a general estimate must be very rough, however, because of the uncertainty in evaluating the relevant parameters. The parameters considered for the present comparative estimate, and their assumed values, are listed in Table 1. Two sets of values have been selected to simulate coherent mass actions (e.g., activity evoked by electrical stimulation or related to coherent interictal spikes) and more dissipated mass actions (e.g., activity evoked by adequate natural stimuli or spontaneous rhythmic activity). The range of likely values was considered for the rise time of dendritic APs and for the fraction of loss current of dendritic EPSPs; in addition, values for very low scatter of APs are given. An equal density of neuronal elements and fibers was assumed. Activations of fiber terminals were not included in this estimate because the details of this process are not known well enough to make the appropriate assumptions (see sect. II*C2a*). The results for fiber APs, dendritic APs, soma APs, EPSPs, and IPSPs are given in the bottom two lines of Table 1.

According to this theoretical estimate, EPSPs cause the largest CSD amplitudes. Their dominance is mainly due to the factor that accounts for the dendritic location of the synapses. Even if the smallest of the corresponding values from the literature is chosen, the EPSPs still cause two to three times larger CSDs than APs in fibers or cell somata. The APs, although having much higher amplitude, are less effective, either because they are very dissipated (fiber APs) or because the fraction of the loss current from the soma is very small (soma APs). During natural activation, soma APs are totally negligible in comparison with EPSPs. This is because of the large cancelling effect, implicit in the biphasic nature of the time function, anti because of the small transfer ratio that must be assumed in this situation. The IPSPs are an order of magnitude less effective than APs or EPSPs. The insignificance of their contribution to CSDs essentially reflects the shallow $\partial V/\partial t$ gradients in comparison with APs and the EPSPs at their dendritic site of generation.

b) Fiber *APs.* The APs in fibers cause larger CSDs than soma APs. Because of their spatial dissipation, however, these CSDs are assessed experimentally only in special cases (see II*C2a*). Fibers larger in diameter and faster in conductance than those considered for the present estimate cause even larger CSDs; however, they are also more dissipated.

TABLE 1. Quantitative estimates of contributions of various types of neuronal activities to current source densities

	Fiber APs		Dendritic APs		Soma APs		EPSPs		IPSPs	
	Coherent	Dissipated	Coherent	Dissipated	Coherent	Dissipated	Fast	Slow	Fast	Slow
Amplitude ΔV (mV)	100	100	100	100	100	100	5[a]	5[a]	5[a]	5[a]
Time to peak ΔT (ms)	0.5	0.5	1.5-5	1.5-5	0.5	0.5	1	10[a]	3	30[a]
Relevant membrane area F (10^{-4} cm^2)[b]	0.09[c]	0.09[c]	0.16[c]	0.16[c]	0.28[d]	0.28[d]	0.28[d]	0.28[d]	0.28[d]	0.28[d]
Loss current/capacitive current = I_{max}/I_c	1.0[e]	1.0[e]	1.0[e]	1.0[e]	0.12[f]	0.12[d]	10[g] (5-20)	10[g] (5-20)	0.7	1.0[f]
Temporal scatter ΔT (ms)	1	10	1	10	1 (0.3)[h]	10	1 (0.3)[h]	10	3	30
Amplitude factor due to $\Delta T = a'$	0.3	0.03	0.7-1.0	0.1-0.3	0.3 (0.8)[h]	0.03	0.5 (0.8)[h]	0.5	0.5	0.5
Spatial scatter Δz (μm)	ND	ND	ND	ND	100	100	100	100	100	100
Amplitude factor due to $\Delta z = b'$	0.1[k]	0.1[k]	0.33[k]	0.33[k]	0.26	0.26	0.26	0.35	0.32	0.36
Transfer ratio = c[l]	1	1	0.7	0.3	0.7	0.3	1	1	1	1
Relative CSD amplitude $= \frac{\Delta V}{\Delta t} \cdot$ area $\mathbf{F} \cdot \frac{I_{max}}{I_c} \cdot a \cdot b \cdot c$										
Averages	0.54	0.05	1.23	0.11	0.36 (0.96)[h]	0.02	1.82 (2.91)[h]	0.25	0.05	0.01
Ranges	ND	ND	0.74-1.72	0.10-0.11	ND	ND	0.91-3.60	0.12-0.49	ND	ND

Parameters were seldcted to simulate electrical (coherent) and natural (dissipated) activation of an ensemble. APs, action potentials; EPSPs, excitatory postsynaptic potentials; IPSPs, inhibitory postsynaptic potentials; CSD, current source density; ND, no data. [a]See refs. 37, 41, 56, 210,318. [b]Relevant membrane area F is defined by $\mathbf{I}_m = c_m \mathbf{d}V/dt$, where maximum capacity $c_m = 2\ \mu$F/cm^2. [c]For fiber conducting at 1 m/s, 1 μm diam and 300 μm length of instantaneously depolarized segment were assumed. For apical dendrites, 5 pm diam and 100 μm length of instantaneously depolarized segment were assumed (219). [d]Because AP and PSP values are from soma, soma surface is relevant area; soma of 30 μm diam was assumed. [e]See ref. 110. [f]See text. [g]Dendritic location of excitatory synapses is considered (see text). [h]Scatter of only 0.3 ms may be appropriate in some cases of antidromic or strong monosynaptic activation via homogeneous, fast-conducting axons (e.g., refs. 56, 294). [i]See Figure 2*E* and text. [j]Reference value of 30 μm is assumed as depth extent of synaptic region and AP-generating membrane. For soma APs and fast EPSPs a factor of 0.26 was assumed, according to Figure 2*F*. Progressively higher values were assumed for slower PSPs, according to frequency dependence of spatial distribution of passive membrane currents (123). Values are proportional to distances of equivalent neighboring sink/source planes. [k]Spatial dissipation of APs along fibers or apical dendrites is considered; see footnote c. [l]Transfer ratio equals number of APs per stimulus (e.g., refs. 75, 79, 109, 294).

c) Dendritic APs. Dendritic APs cause CSDs comparable in amplitude to the CSDs evoked by excitatory synaptic activations. This theoretical result is in good agreement with experiments. In the hippocampus, where dendritic APs are presumed to occur predominantly (323), the field potentials contain a "population spike" with an amplitude in the same range as the amplitude of the EPSP-related component (7). CSDs from hippocampal slices, evoked by suprathreshold stimulation of the stratum radiatum afferents, consistently show a sink (and corresponding sources above and below) in the depth region of the apical dendrites and the somata of the CA1 neurons. The latency of this sink increases toward the soma at ~0.5 ms/100 μm. The amplitude of this sink is about equal to the amplitude of the sink caused by the synaptic activation (272; W. Zieglgänsberger and U. Mitzdorf, unpublished observations). In the alligator cerebellum, Nicholson and Llinás (219) demonstrated a contribution of dendritic APs to field potentials. There too the amplitudes of the contributions from the dendritic APs and from the synaptic activation are similar. Dendritic APs have also been identified, or proposed, as significant contributors to CSDs in several further studies (153, 161, 295, 313).

d) Inhibitory synaptic activations. According to the present estimate, IPSPs do not contribute significantly to CSDs. Indeed, in most CSD studies of synaptic organizations, no contributions attributable to IPSPs were found in the optic tectum (28, 67, 295, 313), the cerebellum (68, 153), the visual cortex (197, 198), or the hippocampus (102). Minor contributions from IPSPs were identified, or assumed, in studies in the prepyriform cortex (101), the LGN (196), the hippocampus (161), the cerebellum (66, 154), and the neocortex (306). A model calculation of evoked potentials, based on single-unit data from the cat somatosensory cortex (305), yielded a proportion of 5:1 for EPSP- versus IPSP-related components.

Correlations of major CSDs with IPSPs were found in two CSD studies (3, 122). The large-amplitude CSD, which Humphrey (122, 123) definitely attributed to IPSPs, actually does not contradict the present estimate, because it can only be elicited by extremely unnatural stimulation (antidromic train stimulation of the pyramidal tract). The large late CSD evoked in the dentate gyrus by stimulation of the perforant path (3) may be an exceptional example for a significant contribution from inhibitory synaptic activation (at the somata). Quantitatively, however, the contribution of IPSPs to the late CSD could not be assessed in that study, because it could not be segregated from contributions evoked by the late phase of the excitatory synaptic activation and the postspike repolarization (4). IPSPs have definitely been identified as the predominant causes of two pathological spontaneous phenomena [the wave of the spike-wave complex (235, 237), the surface-negative type of the delta wave (268)] and of the second surface-negative wave, which sometimes follows the direct cortical response (DCR) (237).

e) Soma APs. According to the present estimate, soma APs can be ignored totally, if temporally dissipated mass actions are investigated. This result is in agreement with all the earlier correlative studies of EEG waves and

single units (for reviews see refs. 35, 241, 270). Even during coherent activations, however, AP CSDs are still about five times smaller than the EPSP CSDs. Only if the scatter of the APs is very low may their contribution become about equally significant (see Table 1). Eccles (48), in accordance with this result, reviewed electrically evoked potential data from cerebral cortex and reached the conclusion that EPSPs were the most probable causes of all these potentials. Since then, further affirmative data have been obtained. In CSD studies of the LGN and the visual cortex, it was demonstrated that the contributions of APs are usually small, compared with the contributions of synaptic activations (196–198). Among these thalamic and cortical relay stations, the monosynaptic activation of cat area 18 should be the component where APs contribute most, because the latency scatter is very low (0.4 ms; 213, 294, 307, 308), and the involved synapses are located on proximal dendrites (197). To make a quantitative estimate for this activation, single unit-data are available. On double-shock stimulation of the primary afferents, the sink of the second response is reduced by 30% (197; U. Mitzdorf, unpublished results), and the number of corresponding APs is reduced by 56% (G. Neumann, personal communication), which implies a contribution of 54% from the APs. This result from experimental data agrees rather well with the corresponding theoretical value for APs, compared with EPSPs from proximal synapses (0.9:1.4). [According to other experimental results, however, this estimate appears to be too high (see sect. III*A2*).]

Nicholson and Llinás (219) indirectly demonstrate that orthodromically evoked soma APs contribute little to the field potentials. Their model calculation of synaptic activation fits the experimental data from the cerebellum very well, although they did not consider APs in their model. Towe (305) could best fit his evoked-potential data from the cat somatosensory cortex by considering PSPs, not APs, in his model calculations. Furthermore, no component is attributed to soma APs in any CSD study of electrically evoked potentials published to date.

The correlations found in many studies, between single-unit responses and peaks of the evoked potentials (e.g., refs. 71, 99, 253, 320), do not contradict the assumption that EPSPs, not APs, are the main causes of the evoked potentials. Because EPSPs cause the APs, such a correlation is to be expected (see also ref. 63). Also, the studies where the responding cells were found in the same cortical depths as the sinks (314) or the negativities of the field potentials (115) may still be interpreted by the causal relationship between EPSPs and APs. According to the depth of the sinks and the potential negativities in both studies, the activities in question were monosynaptic intracortical activities. Because the afferents mainly contact small stellate cells and pyramidal cells at their proximal dendrites (197), this depth correlation of the monosynaptic activity and the APs is very likely.

Antidromically evoked APs, which occur in most of the deep pyramidal cells of the cat visual cortex after stimulation of the optic radiation, have a latency scatter of ~6 ms (86,106,279,308). In agreement with the theoretical considerations, no contribution of these scattered APs to CSDs was found (197). A CSD component resulting from the antidromic activation of pyramidal tract cells was identified by Humphrey (122, 123). Its amplitude was ~40% of the CSD, which was evoked concomitantly by recurrent excitatory synaptic activation. If the latency scatters (1.5 ms for APs, 6 ms for EPSPs) and the distribution of the cell somata over cortical depth (see ref. 123) are taken into account, a theoretical estimate of the relative sizes of the two contributions agrees well with the experimental results. Antidromic activation of Purkinje cells results in a contribution to the field potential (219) or the CSD (66), which is slightly larger than the concomitantly evoked synaptic activation. Because the latencies of these APs show little scatter, and because the somata of the Purkinje cells are rather precisely aligned, these results conform with the theoretical estimates of Table 1 as well.

f) Summary. The theoretical estimate of the relative contributions from APs, EPSPs, and IPSPs to CSDs (Table 1) is justified by its agreement with many experimental results. It leads to the conclusion that EPSPs are essentially the dominant causes of the CSDs. Correspondingly, most experimental CSD studies were designed to yield information about excitatory synaptic ensemble activities. Most of these studies focused on finding out or confirming physiologically where the afferents terminate in the nucleus or cortex under investigation (23, 28, 64, 65, 102, 141, 153, 154, 186a, 196). In several others the polysynaptic organization of excitatory circuits was investigated with the CSD method (101, 197, 198, 313). The method was also applied to assess effects of deprivation, regeneration, conditioning stimulation, or drugs on excitatory synaptic mass actions (65, 67, 140a, 195, 200, 277, 278, 306).

4. Distinction between *CSD contributions* from *different* types of *neuronal* activity

Although EPSPs are the dominant causes of CSDs, significant contributions from presynaptic activity, APs, or IPSPs may occur. They cannot be ruled out from the onset when studying the mass actions of a nucleus or cortex with the CSD method. Cues for a distinction of the contributions from these different types of activity may come from any field of neuroscience. Here the principal relevant arguments are briefly reviewed.

The most direct help comes from anatomical and single-unit studies about the ensemble under investigation. Data from extra- and intracellular single-unit recordings help to identify CSD components by the argument of temporal coincidence; the latency scatter of individual events helps to estimate the likelihood of summation of the related membrane currents (101,102,123, 140a, 186a, 196, 197, 312). The most important anatomical aspects are the types and degrees of orderliness within the ensemble. Anatomical data may disentangle the ensemble into subgroups of similar elements. The geometries

of these elements, their density, and the degree of their alignment and spatial scatter are essential cues. They help to attribute CSD components according to spatial correlations, according to the succession of events as determined by the circuits, and according to quantitative arguments about summation properties of elements (101, 102, 123, 153, 154, 196–198, 235, 272, 295, 313).

In addition to these sources of information from separate anatomical and physiological studies, essential cues may be obtained by varying the mass actions of the ensemble. Stimulation of the afferents at different locations along their path helps to disentangle the contributions due to fast- and slow-conducting afferents, according to the differential latency changes of the CSD components (196–198, 312, 313). According to their different thresholds, fast- and slow-conducting fibers may further be differentiated by variation of the stimulus strength (141, 312, 313). Train stimuli or double stimuli may help to distinguish between pre- and postsynaptic components, or between mono- and polysynaptic components, according to the differences in their recovery cycles (3, 28, 101, 118, 196–198, 272, 312, 313). Local or systemic application of pharmacological agents, which either attenuate or facilitate specific mechanisms, can help to a'ttribute CSD components according to their amplitude changes caused by the drug (3, 28, 65, 67). [The practices of repetitive stimulation and drug application were already common tools in the pioneering studies of evoked potentials (e.g., refs. 10, 11, 18, 43, 60, 186).]

III. CURRENT SOURCE-DENSITY ANALYSIS OF EVOKED POTENTIALS IN CAT VISUAL CORTEX

This description of an experimental application illustrates the theoretical arguments given above. In two series of studies (193, 194, 197, 200), field potentials evoked by electrical and visual stimuli were recorded in primary visual areas 17 and 18 of the cat cortex (acute experiments; anesthesia: pentobarbital and/or N_2O) and were subsequently subjected to CSD analysis. The use of different types of stimuli and comparisons with anatomical and single-unit data helped to interpret the CSDs. With the wealth of known anatomical and physiological facts about the cat visual cortex, it was possible to identify the origins of the sinks and sources. Their spatiotemporal distributions revealed new aspects of the intracortical processing of afferent information. The main arguments and conclusions of these experimental studies are outlined in this section.

A. Electrically Evoked CSDs

Most of the electrically evoked field potentials were recorded with one micropipette, which was successively placed at different cortical depths. The recordings were made equidistantly at $\Delta z = 50$ or 100 pm. From these profiles, the one-dimensional CSDs were calculated with a differentiation grid of $n \cdot \Delta z = 200\ \mu m$ (see *Eq. 8*), while the intracortical conductivity was assumed constant (see sect. II*A*). An example of such a potential profile and the corresponding CSD profile is given in Figure 3*A*, B.

1. *Relation* between potentials and CSDs

A cursory comparison of the two profiles in Figure 3 already demonstrates the localizing effect of the CSD method. Whereas the various peaks of the field-potential profile are widely dissipated over depth and have large amplitudes even in the white matter below the cortex, the CSD profile is well structured and reveals discrete events. In the potential profiles, some of these local events are totally hidden among large-amplitude far-field components (e.g., component f in Fig. 3B: the large sink and the corresponding sources above and below create a closed-field component, which is barely recognizable in the potential profile).

In area 18, electrical stimulation of the primary afferents evokes a potential that is roughly mirror symmetrical at the surface and in the white matter (see ref. 197). Therefore the generators of this potential are located between these two depths (see sect. II*A*). In area 17, on the other hand, the surface potential is very small, whereas the white matter potential has large-amplitude peaks (see Fig. 3*A*). The asymmetry indicates that large far-field components contribute to this potential. These probably originate in other regions of area 17. This area occupies roughly a hemisphere at the occipital pole and is evenly activated by stimulation of the primary afferents. The occipital pole, viewed as a whole therefore generates a "closed field" (140), with a large-amplitude potential at the center of the sphere (i.e., in the white matter) and only minor deflections at the surface (i.e., at the cortical surface).

Because the surface potential over area 17 is the rather arbitrary and small result of the superposition of the large locally generated component and the large (inverted) far-field component from "opposite" regions of area 17, it does not contain any useful information. The peaks of the surface potential over area 18, on the other hand, can be attributed to underlying local events (197). This surface potential, which is essentially caused by activity within area 18, has erroneously been attributed to area 17 in earlier works (for review see ref. 36).

2. *Interpretation* of CSDs

To identify the neuronal activity causing the sink and source peaks within areas 17 and 18 (e.g., Fig. 3*B*), stimuli were applied in the optic radiation (OR), in the optic chiasm (OX), at the optic nerves (ON), and within the cortical areas themselves. These stimuli were presented as double shocks with a 20-ms interstimulus time, and their strength was varied. In addition,

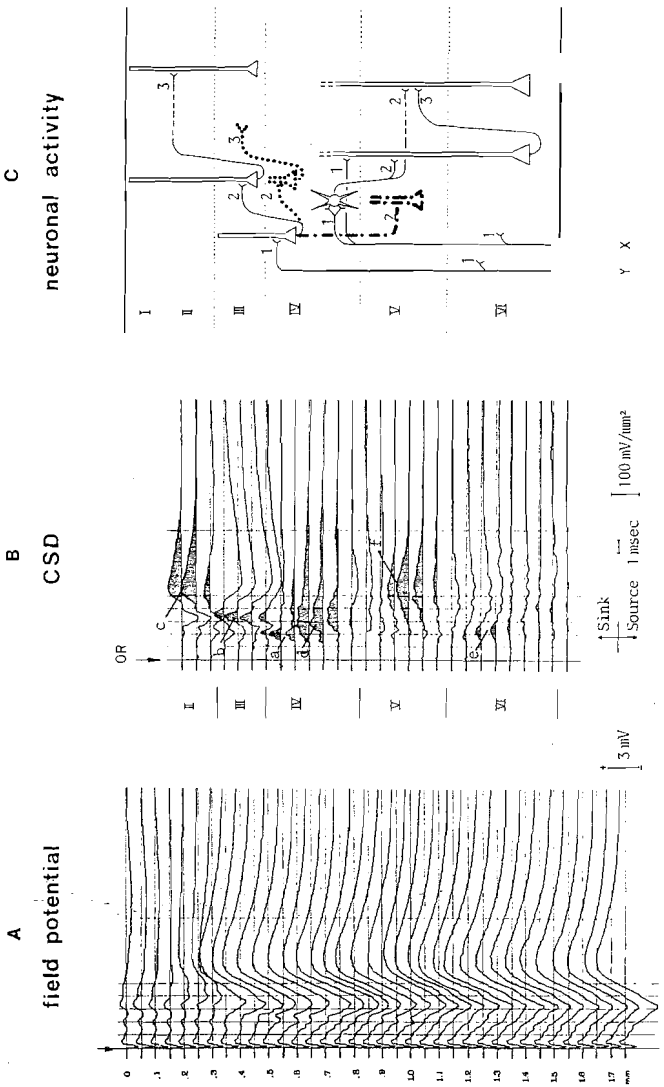

the effects of two pharmacological agents (picrotoxin and pentobarbital) were investigated.

Comparison of OR-, OX-, and ON-evoked CSDs in area 18 confirmed that this area is activated essentially by the fast-conducting Y-type afferents (264, 294, 308). On stimulation of the afferents at the farther sites, the CSD as a whole was delayed; however, it was not more dissipated. The CSDs in area 17, on the contrary, were more dissipated. According to their differential latency increases, the components could be attributed either to Y-type activity mediated by the fast-conducting afferents or to X-type activity mediated by the slower-conducting afferents. The earliest sinks and sources of each group could then be attributed to monosynaptic activity and all later components to polysynaptic activity mediated by intracortical connections.

The CSDs evoked by the second of the double shock in OR are consistent with this latter point; when the second afferent volley arrives in cortex, the cells are under strong inhibitory influence due to the first activation (213, 279, 307, 308). This inhibition does not affect the monosynaptic activation, but it prevents the generation of APs in many cells. Accordingly, the sinks and sources, which had been attributed to monosynaptic activation, were still present in these CSDs; those components that had been attributed to polysynaptic activation, however, were drastically reduced or totally missing. The attribution of two sink/source components to polysynaptic activities, according to the above arguments, could further be confirmed by intracortical stimulation. Direct stimulation of cortex several millimeters distant from the recording site evoked predominantly those polysynaptic components. In addition, this result implies that long-distance connections are involved in the mediation of these polysynaptic activations.

Picrotoxin and pentobarbital were applied systemically to investigate

FIG. 3. *A:* field potential in primary visual cortex (area 17) of cat evoked by electrical stimulation of optic radiation (*arrow*). Stimulus was preceded by stabilizing stirnulation of reticular formation (see ref. 197). Each *trace* is average of 20 responses. Distance between adjacent recordings is 50 pm. Profile was obtained by successive recordings with 1 micropipette. B: current source-density (CSD) distribution obtained from potential profile in A, according to Equation 8, with differentiation grid of $n \cdot \Delta z$ = 200 pm. According to *Equation* a', highest and lowest regions of recording range are missing in CSD profile. Sinks, corresponding to active excitatory postsynaptic potential currents, are shaded At *left*, depth regions of cortical laminae are indicated. Sinks a, b, and c reflect mono-, di-, and trisynaptic Y-type activity; sinks d and f reflect mono-, di-, and trisynaptic X-type activity; sink e reflects Y-type and X-type monosynaptic activity. *C*: schematic diagram of successive intracortical excitatory relay stations as well as cell types involved, as suggested by CSD in B and similar findings (see sect. IIIA). Three main pathways along which afferent activity is relayed within the visual cortex were revealed (long-distance connections are indicated by dashed lines; numbers indicate whether activations are mono-, di-, or trisynaptic). First pathway transmits afferent Y-type activity from upper layer IV to layer III and then to layer II. Second pathway relays afferent X-type activity from lower layer IV to layer V, where mainly lamina VI pyramidal cells are contacted (di- and trisynaptically). Along third pathway (dotted *connections*), Y-type afferent activity is relayed within layer IV and then projected to layer III. Y-type activation of lamina V cells, as suggested by single-unit studies, is also indicated (dash-dot connections).

physiological Study of the Synaptic Mechanisms which Affect the Excitability of the Granule Cells of the Dentate Gyrus in the Rabbit (PhD thesis). London: Univ. of London, 1977.
5. AMASSIAN, V. E., H. J. WALLER, AND J. MACY, JR. Neural mechanism of primary somatosensory evoked potential. *Ann. NY Acad. Sci.* 112: 5–32, 1964.
6. ANDERSEN, P., AND S. A. ANDERSSON. *Physiological Basis of the Alpha-Rhythm.* New York: Appleton-Century-Crofts, 1968.
7. ANDERSEN, P., T. V. P. BLISS, AND K. K. SKREDE. Unit analysis of hippocampal population spikes. *Exp. Brain Res.* 13: 208–221, 1971.
8. ARAKI, T., AND C. A. TERZUOLO. Membrane currents in spinal motoncurons associated with the action potential and synaptic activity. *J. Neurophysiol.* 25: 772–789, 1962.
9. BARRETT, J. N., AND W. E. CRILL. Influence of dendritic location and membrane properties on the effectiveness of synapses on cat motoneurones. *J. Physiol. London* 293: 325–345, 1974.
10. BARTLEY, S. H. Action potentials of the optic cortex under the influence of strychnine. *Am. J. Physiol.* 103: 203–212, 1933.
11. BARTLEY, S. H. Temporal and spatial summation of extrinsic impulses with the intrinsic activity of the cortex. *J. Cell. Comp. Physiol.* 8: 41–62, 1936.
12. BARTLEY, S. H., AND G. H. BISHOP. The cortical response to stimulation of the optic nerve in the rabbit. *Am. J. Physiol.* 103: 159–172, 1933.
13. BAŞAR, E. *EEG-Brain Dynamics. Relation Between EEG and Brain Evoked Potentials.* Amsterdam: Elsevier/North-Holland, 1980.
14. BERGER, H. Über das Elektrenkephalogramm des Menschen. *Arch. Psychiatr. Nervenkr.* 87: 527–570, 1929.
15. BERKLEY, M. A., AND R. BUSH. Intracortical processing of visual contour information in cats. *Exp. Brain Res.* 50: 397–407, 1983.
16. BERMAN, N., B. R. PAYNE, D. R. LABAR, AND E. H. MURPHY. Functional organization of neurons in cat striate cortex: variations in ocular dominance and receptive-field type with cortical laminae and location in visual field. *J. Neurophysiol.* 48: 1362–1377, 1982.
17. BIGNALL, K. E., AND L. T. RUTLEDGE. Origin of a photically evoked afterdischarge in cat visual cortex. *J. Neurophysiol.* 27: 1048–1062, 1964.
18. BISHOP, G. H. Cyclic changes in excitability of the optic pathway of the rabbit. *Am. J. Physiol.* 103: 213–224, 1933.
19. BISHOP, P. O., W. BURKE, AND R. DAVIS. The identification of single units in central visual pathways. *J. Physiol. London* 162: 409–431, 1962.
20. BISTI, S., G. IOSIF, AND P. STRATA. Suppression of inhibition in the cerebellar cortex by picrotoxin and by bicuculline. *Brain Res.* 28: 591–593, 1971.
21. BOWKER, R. M., AND A. R. MORRISON. The startle reflex and PGO spikes. *Brain Res.* 102: 185–190, 1976.
22. BRAZIER, M. A. B., K. F. KILLAM, AND A. J. HANCE. The reactivity of the nervous system in the light of the past history of the organism. In: *Sensory Communication*, edited by W. A. Rosenblith. New York: MIT Press, 1961, p. 699–716.
23. BRECKOW, J., K. KALMRING, AND R. ECKHORN. Multichannel-recordings and real-time current source density (CSD) analysis in the central nervous system of insects. *Biol. Cybern.* 45: 115–121, 1982.
24. BROOKS, D. C., AND M. D. GERSHON. Eye movement potentials in the oculomotor and visual systems of the cat: a comparison of reserpine induced waves with those present during wakefulness and rapid eye movement sleep. *Brain Res.* 27: 223–239, 1971.
25. BUSER, P., AND F. E. HORVATH. Thalamo-caudate-cortical relationships in synchronized activity. II. Further differentiation between spindle systems by cooling and lesions in the mesencephalon. *Brain Res.* 39: 43–60, 1972.
26. CALVET, J., M. C. CALVET, AND J. SCHERRER. Étude stratigraphique corticale de l'activité EEG spontanée. *Electroencephalogr. Clin. Neurophysiol.* 17: 109–125, 1964.
27. CAVINESS, V. S., JR., AND D. O. FROST. Tangential organization of thalamic projections to the neocortex in the mouse. *J. Comp. Neurol.* 134: 335–367, 1980.
28. CHUNG, S. H., T. V. P. BLISS, AND M. J. KEATING. The synaptic organization of optic afferents in the amphibian tectum. *Proc. R. Soc. London Ser. B* 187: 421–447, 1974.
29. CLELAND, B. G., AND C. ENROTH-CUGELL. Quantitative aspects of gain and latency in the cat retina. *J. Physiol. London* 206: 73–91, 1970.
30. COHEN, M. W. Glial potentials and their contribution to extracellular recordings. In: *Handbook of Electroencephalography and Clinical Neurophysiology*, edited by O. Creutzfeldt. Amsterdam: Elsevier, 1974, vol. 2B, p. 43–60.
31. COLONNIER, M. Synaptic patterns of different cell types in the different laminae of the cat visual cortex. An electron microscope study. *Brain Res.* 9: 268–287, 1968.
32. COLONNIER, M., AND S. ROSSIGNOL. Heterogeneity of the cerebral cortex. In: *Basic Mechanisms of Epilepsy*, edited by H. H. Jasper, A. A. Ward, and A. Pope. Boston, MA: Little, Brown, 1969, p. 29–40.
33. COWAN, W. M., AND M. CUENOD (editors). *The Use of Axonal Transport for Studies of Neuronal Connectivity.* New York: Elsevier, 1975.
34. CREUTZFELDT, O. D., L. J. GAREY, R. KURODA, AND J.-R. WOLFF. The distribution of degenerating axons after small lesions in the intact and isolated visual cortex of the cat. *Exp. Brain Res.* 27: 419–440, 1977.
35. CREUTZFELDT, O., AND J. HOUCHIN. Neuronal basis of EEG waves. In: *Handbook of Electroencephalography and Clinical Neurophysiology*, edited by A. Rémond and O. Creutzfeldt. Amsterdam: Elsevier, 1974, vol. 2C, p. 5–55.
36. CREUTZFELDT, O. D., AND U. KUHNT. Electrophysiological and topographical distribution of visual evoked potentials in animals. In: *Handbook of Sensory Physiology. Visual Centers in the Brain*, edited by R. Jung. Berlin: Springer-Verlag, 1973, vol. VII, pt. 3/B, p. 595–646.
37. CREUTZFELDT, O. D., U. KUHNT, AND L. A. BENEVENTO. An intracellular analysis of visual cortical neurones to moving stimuli: responses in a co-operative neuronal network. *Exp. Brain Res.* 21: 251–274, 1974.
38. CREUTZFELDT, O., R. SPEHLMANN, AND D. LEHMANN. Veränderungen der Neuronaktivität des visuellen Cortex durch Reizung der Substantia reticularis mesencephali. In: *Neurophysiologie und Psychophysik des visuellen Systems*, edited by R. Jung and H. Kornhuber. Berlin: Springer-Verlag, 1961, p. 351–363.
39. CREUTZFELDT, O., AND G. STRUCK. Neurophysiologic und Morphologie der chronisch isolierten Cortexinsel der Katze: Hirnpotentiale und Neuronenaktivität einer isolierten Nervenzellpopulation ohne afferente Fasern. *Arch. Psychiatr. Nervenkr.* 203: 708–731, 1962.
40. CREUTZFELDT, O. D., S. WATANABE, AND H. D. LUX. Relations between EEG phenomena and potentials of single cortical cells. I. Evoked responses after thalamic and epicortical stimulation. *Electroencephalogr. Clin. Neurophysiol.* 20: 1–18, 1966.
41. CREUTZFELDT, O. D., S. WATANABE, AND H. D. LUX. Relations between EEG phenomena and potentials of single cortical cells. II. Spontaneous and convulsoid activity. *Electroencephalogr. Clin. Neurophysiol.* 20: 19–37, 1966.

42. CRILL, W. E., AND P. C. SCHWINDT. Active currents in mammalian central neurons. *Trends Neurosci.* 6: 236–240, 1983.
43. CURTIS, H. J. An analysis of cortical potentials mediated by the corpus callosum. *J. Neurophysiol.* 3: 414–422, 1940.
44. DANIELS, J. D., AND J. D. PETTIGREW. A study of inhibitory antagonism in cat visual cortex. *Brain Res.* 93: 41–62, 1975.
45. DOTY, R. W. Potentials evoked in cat cerebral cortex by diffuse and punctiform photic stimuli. *J. Neurophysiol.* 21: 437–464, 1958.
46. DOTY, R. W., D. S. KIMURA, AND G. J. MORGENSON. Photically and electrically elicited responses in the central visual system of the squirrel monkey. *Exp. Neurol.* 10: 19–51, 1964.
47. DOTY, R. W., P. D. WILSON, J. R. BARTLETT, AND J. PECCI-SAAVEDRA. Mesencephalic control of lateral geniculate nucleus in primates. I. Electrophysiology. *Exp. Brain Res.* 18: 189–203, 1973.
47a. EBERSOLE, J. S., AND A. B. CHATT. Laminar interactions during neocortical epileptogenesis. *Brain Res.* 298: 253–271, 1984.
47b. EBERSOLE, J. S., AND B. J. KAPLAN. Intracortical evoked potentials of cats elicited by punctate visual stimuli in receptive field peripheries. *Brain Res.* 224: 160–164, 1981.
48. ECCLES, J. C. Interpretation of action potentials evoked in the cerebral cortex. *Electroencephalogr. Clin. Neurophysiol.* 3: 449–464, 1951.
49. ECCLES, J. C. *The Physiology of Synapses.* Berlin: Springer-Verlag, 1964.
50. ECCLES, J. C. The modular operation of the cerebral neocortex considered as the material basis of mental events. *Neuroscience* 6: 1839–1856, 1981.
51. ELGER, C. E., E.-J. SPECKMANN, O. PROHASKA, AND H. CASPERS. Pattern of intracortical potential distribution during focal interictal epileptiform discharges (FIED) and its relation to spinal field potentials in the rat. *Electroencephalogr. Clin. Neurophysiol.* 51: 393–402, 1981.
52. ELUL, R. The genesis of the EEG. *Int. Rev. Neurobiol.* 15: 227–272, 1972.
53. EMSON, P. C., AND O. LINDVALL. Distribution of putative neurotransmitters in the neocortex. *Neuroscience* 4: 1–30, 1979.
54. EVARTS, E. V. Photically evoked responses in visual cortex units during sleep and waking. *J. Neurophysiol.* 26: 229–248, 1963.
55. EVARTS, E. V. Unit activity in sleep and wakefulness. In: *The Neurosciences*, edited by G. C. Quarton, T. Melnechuck, and F. O. Schmitt. New York: Rockefeller Univ. Press, 1967, p. 545–556.
56. EYSEL, U. T. Quantitative studies of intracellular postsynaptic potentials in the lateral geniculate nucleus of the cat with respect to optic tract stimulus response latencies. *Exp. Brain Res.* 25: 469–486, 1976.
57. FERSTER, D., AND S. LEVAY. The axonal arborizations of lateral geniculate neurons in the striate cortex of the cat. *J. Comp. Neurol.* 182: 923–944, 1978.
58. FESSARD, A. The role of neuronal networks in sensory communications within the brain. In: *Sensory Communication*, edited by W. A. Rosenblith. New York: MIT Press, 1961, p. 585–606.
59. FISKEN, R. A., L. J. GAREY, AND T. P. S. POWELL. The intrinsic, association and commissural connections of area 17 of the visual cortex. *Philos. Trans. R. Soc. London Ser. B* 272: 487–536, 1975.
60. FORBES, A., AND B. R. MORISON. Cortical responses to sensory stimulation under deep barbiturate narcosis. *J. Neurophysiol.* 2: 112–128, 1939.
61. FOSTER, J. A. Intracortical origin of recruiting responses in the cat cortex. *Electroencephalogr. Clin. Neurophysiol.* 48: 639–653, 1980.
62. FOX, S. S. Evoked potential, coding and behavior. In: *The Neurosciences. Second Study Program*, edited by F. O. Schmitt. New York: Rockefeller Univ. Press, 1970, p. 243–259.
63. FOX, S. S., AND J. H. O'BRIAN. Duplication of evoked potential waveform by curve of probability of firing of a single cell. *Science* 147: 888–890, 1965.
64. FREEMAN, B., AND W. SINGER. The direct and indirect visual inputs to the superficial layers of the cat superior colliculus: a current source-density analysis of electrically evoked potentials. *J. Neurophysiol.* 49: 1075–1091, 1983.
65. FREEMAN, J. A. Possible regulatory function of acetylcholine receptor in maintenance of retinotopic synapses. *Nature London* 269: 218–222, 1977.
66. FREEMAN, J. A., AND C. NICHOLSON. Experimental optimization of current source-density technique for anuran cerebellum. *J. Neurophysiol.* 38: 369–382, 1975.
67. FREEMAN, J. A., J. T. SCHMIDT, AND R. E. OSWALD. Effect of α-bungarotoxin on retinotectal synaptic transmission in the goldfish and the toad. *Neuroscience* 5: 929–942, 1980.
68. FREEMAN, J. A., AND J. STONE. A technique for current density analysis of field potentials and its application to the frog cerebellum. In: *Neurobiology of Cerebellar Evolution and Development*, edited by R. Llinás. Chicago, IL: Am. Med. Assoc., 1969, p. 421–430.
69. FREEMAN, W. J. *Mass Action in the Nervous System.* New York: Academic, 1975, p. 175 ff.
70. FREYGANG, W. H., JR., AND W. M. LANDAU. Some relations between resistivity and electrical activity in the cerebral cortex of the cat. *J. Cell. Physiol.* 45, Suppl.: 377–392, 1955.
71. FROMM, G. H., AND H. W. BOND. The relationship between neuron activity and cortical steady potentials. *Electroencephalogr. Clin. Neurophysiol.* 22: 159–166, 1967.
72. FROST, D. O., AND V. S. CAVINESS, JR. Radial organization of thalamic projections to the neocortex of the mouse. *J. Comp. Neurol.* 194: 369–393, 1980.
73. FROST, J. D., JR. EEG-intracellular potential relationship in isolated cerebral cortex. *Electroencephalogr. Clin. Neurophysiol.* 24: 434–443, 1968.
74. FUKADA, Y., AND H. SAITO. The relationship between response characteristics to flicker stimulation and receptive field organization in the cat's optic nerve fibers. *Vision Res.* 11: 227–240, 1971.
75. FUKADA, Y., AND J. STONE. Evidence of differential inhibitory influences on X- and Y-type relay cells in the eat's lateral geniculate nucleus. *Brain Res.* 113: 188–196, 1976.
76. FUSTER, J. M., AND R. F. DOCTER. Variations of optic evoked potentials as a function of reticular activity in rabbits with chronically implanted electrodes. *J. Neurophysiol.* 25: 324–336, 1962.
77. GALAMBOS, R., AND S. A. HILLYARD. Electrophysiological approaches to human cognitive processing. *Neurosci. Res. Program Bull.* 20: 145–265, 1981.
78. GALINDO, A. GABA-picrotoxin interaction in the mammalian central nervous system. *Brain Res.* 14: 763–767, 1969.
79. GALLETTI, C., M. G. MAIOLI, S. SQUATRITO, AND E. RIVA SANSEVERINO. Single unit responses to visual stimuli in cat cortical areas 17 and 18. I. Responses to stationary stimuli of variable intensity. *Arch. Ital. Biol.* 117: 208–230, 1979.
80. GALLETTI, C., S. SQUATRITO, M. G. MAIOLI, AND E. RIVA SANSEVERINO. Single unit responses to visual

stimuli in cat cortical areas 17 and 18. II. Responses to stationary stimuli of variable duration. *Arch. Ital. Biol.* 117: 231–247, 1979.

81. GARDNER-MEDWIN, A. R. Membrane transport and solute migration affecting the brain cell microenvironment. *Neurosci. Res. Program Bull.* 18: 208–226, 1980.
82. GAREY, L. J., E. G. JONES, AND T. P. S. POWELL. Interrelationships of striate and extrastriate cortex with the primary relay sites of the visual pathway. *J. Neurol. Neurosurg. Psychiatry* 31: 135–157, 1968.
83. GAREY, L. J., AND T. P. S. POWELL. The projection of the lateral geniculate nucleus upon the cortex in the cat. *Proc. R. Soc. London Ser. B* 169: 107–126, 1967.
84. GAREY, L. J., AND T. P. S. POWELL. An experimental study of the termination of the lateral geniculo-cortical pathway in the cat and monkey. *Proc. R. Soc. London Ser. B* 179: 41–63, 1971.
85. GEISERT, E. E., JR. Cortical projections of the lateral geniculate nucleus in the cat. *J. Comp. Neurol.* 190: 793–812, 1980.
86. GILBERT, C. D. Laminar differences in receptive field properties of cells in primary visual cortex. *J. Physiol. London* 268: 391–421, 1977.
87. GILBERT, C. D., AND J. P. KELLY. The projections of cells in different layers of the cat's visual cortex. *J. Comp. Neurol.* 163: 81–106, 1975.
88. GILBERT, C. D., AND T. N. WIESEL. Morphology and intracortical projections of functionally characterised neurones in the cat visual cortex. *Nature London* 280: 120–125, 1979.
89. GILBERT, C. D., AND T. N. WIESEL. Clustered intrinsic connections in cat visual cortex. *Neuroscience* 3: 1116–1133, 1983.
90. GINSBURG, A. P. Psychological correlates of a model of the human visual system. *IEEE Trans. Aerosp. Electron. Syst.*: 283–290, 1971. (Proc. 1971 Natl. Aerosp. Electronics Conf.)
91. GLENN, L. L., J. HADA, J. P. ROY, M. DECHÊNES, AND M. STERIADE. Anterograde tracer and field potential analysis of the neocortical layer I projection from nucleus ventralis medialis of the thalamus in cat. *Neuroscience* 7: 1861–1877, 1982.
92. GOLDRING, S., J. S. O'LEARY, T. G. HOLMES, AND M. J. JERVA. Direct response of isolated cerebral cortex of cat. *J. Neurophysiol.* 24: 633–650, 1961.
93. GOTTLIEB, D. I., AND W. M. COWAN. On the distribution of axonal terminals containing spheroidal and flattened synaptic vesicles in the hippocampus and dentate gyrus of the rat and cat. *Z. Zellforsch. Mikrosk. Anat.* 129: 413–429, 1972.
94. GRINVALD, A., A. MANKER, AND M. SEGAL. Visualisation of the spread of activity in rat hippocampal slices by voltage-sensitive optical probes. *J. Physiol. London* 333: 269–291, 1982.
95. GROSSMAN, R. G., AND T. L. HAMPTON. Depolarization of cortical glial cells during electrocortical activity. *Brain Res.* 11: 316–324, 1968.
96. GROSSMAN, R. G., L. WHITESIDE, AND T. L. HAMPTON. The time course of evoked depolarization of cortical glial cells. *Brain Res.* 14: 401–415, 1969.
97. GRUNDFEST, H. Synaptic and ephaptic transmission. In: *The Neurosciences*, edited by G. L. Quarton, T. Melnechuck, and F. O. Schmitt. New York: Rockefeller Univ. Press, 1967, p. 353–372.
98. GRÜSSER, O.-J., AND C. RABELO. Reaktionen einzelner retinaler Neurone auf Lichtblitze. I. Einzelblitze und Lichtblitze wechselnder Frequenz. *Pluegers Arch.* 265: 501–525, 1958.
99. GRÜTZNER, A., O.-J. GRÜSSER, AND G. BAUMGARTNER. Reaktionen einzelner Neurone im optischen Cortex der Katze nach elektrischer Reizung des Nervus opticus. *Arch. Psychiatr. Nervenkr.* 197: 377–404, 1958.
100. GUMNIT, R. J., H. MATSUMOTO, AND C. VASCONETTI. DC activity in the depth of an experimental epileptic focus. *Electroencephalogr. Clin. Neurophysiol.* 28: 333–339, 1970.
101. HABERLY, L. B., AND G. M. SHEPHERD. Current density analysis of summed evoked potentials in opossum prepyriform cortex. *J. Neurophysiol.* 36: 789–803, 1973.
102. HABETS, A. M. M. C., F. H. LOPES DA SILVA, AND W. J. MOLLEVANGER. An olfactory input to the hippocampus of the cat: field potential analysis. *Brain Res.* 182: 47–64, 1980.
103. HAGINS, W. A. Electrical signs of information flow in photoreceptors. *Cold Spring Harbor Symp. Quant. Biol.* 30: 403–418, 1965.
104. HAGINS, W. A., R. D. PENN, AND S. YOSHIKAMI. Dark current and photo-current in retinal rods. *Biophys. J.* 10: 380–412, 1970.
105. HAMMOND, P., AND D. M. MACKAY. Differential responsiveness of simple and complex cells in cat striate cortex to visual texture. *Exp. Brain Res.* 30: 275–296, 1977.
106. HARVEY, A. R. Characteristics of corticothalamic neurons in area 17 of the cat. *Neurosci. Lett.* 7: 177–181, 1978.
107. HEINEMANN, U., AND H. D. LUX. Ionic changes during experimentally induced epilepsies. In: *Progress in Epilepsy*, edited by F. C. Rose. London: Pitman, 1983, p. 87–103.
108. HERKENHAM, M. Laminar organization of thalamic projections to the rat neocortex. *Science* 207: 532–535, 1980.
109. HERZ, A., O. CREUTZFELDT, AND J. FUSTER. Statistische Eigenschaften der Neuronaktivität im ascendierenden visuellen System. *Kybernetik* 2: 61–71, 1964.
110. HODGKIN, A. L., AND A. F. HUXLEY. A quantitative description of membrane currents and its application to conduction and excitation in nerve. *J. Physiol. London* 117: 500–544, 1952.
111. HOELTZELL, P. B., AND R. W. DYKES. Conductivity in the somatosensory cortex of the cat—evidence for cortical anisotropy. *Brain Res.* 177: 61–82, 1979.
112. HOELTZELL, P. B., AND R. W. DYKES. Current source density analysis of the somatosensory evoked potential in the cat. *Soc. Neurosci. Abstr.* 8: 925, 1982.
113. HOFFMANN, K.-P., AND J. STONE. Conduction velocity of afferents to cat visual cortex: a correlation with cortical receptive field properties. *Brain Res.* 32: 460–466, 1971.
114. HOLLÄNDER, H., AND H. VANEGAS. The projection from the lateral geniculate nucleus onto the visual cortex in the cat. *J. Comp. Neurol.* 173: 519–536, 1977.
115. HOLMES, O., AND A. D. SHORT. Interaction of cortical evoked potentials in the rat. *J. Physiol. London* 209: 433–452, 1970.
116. HOLMES, O., AND G. T. SUNDERLAND. Generator sites in acute epileptic foci (abstr.). *Electroencephalogr. Clin. Neurophysiol.* 44: 132, 1978.
117. HORVATH, F. E., AND P. BUSER. Thalamo-caudate-cortical relationships in synchronized activity. I. Differentiation between ventral and dorsal spindle systems. *Brain Res.* 39: 21–41, 1972.
118. HOWLAND, B., J. Y. LETTVIN, W. S. MCCULLOCH, W. PITTS, AND P. D. WALL. Reflex inhibition by dorsal root interaction. *J. Neurophysiol.* 18: 1–17, 1955.

119. HUBEL, D. H., AND T. N. WIESEL. Receptive fields, binocular interaction and functional architecture in the cat's visual cortex. *J. Physiol. London* 160: 106–154, 1962.
120. HUBEL, D. H., AND T. N. WIESEL. Receptive fields and functional architecture in two nonstriate visual areas (18 and 19) of the cat. *J. Neurophysiol.* 28: 229–289, 1965.
121. HUGHES, J. R. Responses from the visual cortex of unanesthetized monkeys. *Int. Rev. Neurobiol.* 7: 99–152, 1965.
122. HUMPHREY, D. R. Re-analysis of the antidromic cortical response. I. Potentials evoked by stimulation of the isolated pyramidal tract. *Electroencephalogr. Clin. Neurophysiol.* 24: 116–129, 1968.
123. HUMPHREY, D. R. Re-analysis of the antidromic cortical response. II. On the contribution of cell discharge and PSPs to the evoked potentials. *Electroencephalogr. Clin. Neurophysiol.* 25: 421–442, 1968.
124. IANSEK, R., AND S. J. REDMAN. An analysis of the cable properties of spinal motoneurones using a brief intracellular current pulse. *J. Physiol. London* 234: 613–636, 1973.
125. IANSEK, R., AND S. J. REDMAN. The amplitude, time course and charge of unitary excitatory post-synaptic potentials evoked in spinal motoneurone dendrites. *J. Physiol. London* 234: 665–688, 1973.
126. JACKSON, J. D. *Classical Electrodynamics*. New York: Wiley, 1975, p. 38–40.
127. JAMI, L. Patterns of cortical population discharges during metrazol-induced seizures in cats. *Electroencephalogr. Clin. Neurophysiol.* 32: 641–654, 1972.
128. JEANNEROD, M., AND K. SAKAI. Occipital and geniculate potentials related to eye movements in unanaesthetized cat. *Brain Res.* 19: 361–377, 1970.
129. JEFFREYS, D. A. The physiological significance of pattern visual evoked potentials. In: *Visual Evoked Potentials in Man: New Developments*, edited by J. E. Desmedt. Oxford, UK: Clarendon, 1977, p. 134–167.
130. JOHN, E. R. Electrophysiological studies of conditioning. In: *The Neurosciences*, edited by G. C. Quarton, T. Melnechuck, and F. O. Schmitt. New York: Rockefeller Univ. Press, 1967, p. 690–704.
131. JOHNSTON, D. Passive cable properties of hippocampal CA3 pyramidal neurons. *Cell Mol. Neurobiol.* 1: 41–55, 1981.
132. JOHNSTON, D., AND T. H. BROWN. Giant synaptic potential hypothesis for epileptic activity. *Science* 211: 294–297, 1981.
133. JONES, E. G. Functional subdivision and synaptic organization of the mammalian thalamus. In: *Neurophysiology IV*, edited by R. Porter. Baltimore, MD: University Park, 1981, vol. 25, 173–245. (Int. Rev. Physiol. Ser.)
134. KARMOS, G., M. MOLNÁR, AND V. CSÉPE. A new multielectrode for chronic recording of intracranial field potentials in the cat. *Physiol. Behav.* 29: 567–571, 1982.
135. KASAMATSU, T. Maintained and evoked unit activity in the mesencephalic reticular formation of the freely moving cat. *Exp. Neurol.* 28: 450–470, 1970.
136. KASAMATSU, T., AND W. R. ADEY. Visual cortical units associated with phasic activity in REM sleep and wakefulness. *Brain Res.* 55: 323–331, 1973.
137. KATCHALSKY, A. K., V. ROWLAND, AND R. BLUMENTHAL. Dynamic patterns of brain cell assemblies. *Neurosci. Res. Program Bull.* 12: 1–187, 1974.
138. KAWAMURA, K. Corticocortical fiber connections of the cat cerebrum. III. The occipital region. *Brain Res.* 51: 41–60, 1973.
139. KLEE, M. R. Different effects on the membrane potential of motor cortex units after thalamic and reticular stimulation. In: *The Thalamus*, edited by D. P. Purpura and M. D. Yahr. New York: Columbia Univ. Press, 1966, p. 287–317.
140. KLEE, M., AND W. RALL. Computed potentials of cortically arranged populations of neurons. *J. Neurophysiol.* 40: 647–666, 1977.

140a. KOMATSU, Y., K. TOYAMA, J. MAEDA, AND H. SAKAGUCHI. Long-term potentiation investigated in a slice preparation of striate cortex of young kittens. *Neurosci. Lett.* 26: 269–274, 1981.

141. KORNACKER, K. Some properties of the afferent pathway in the frog corneal reflex. *Exp. Neurol.* 7: 224–239, 1963.
142. KOSTOPOULOS, G., M. AVOLI, A. PELLEGRINI, AND P. GLOOR. Laminar analysis of spindles and spikes of the spike and wave discharge of feline generalized penicillin epilepsy. *Electroencephalogr. Clin. Neurophysiol.* 53: 1–13, 1982.
143. KRAUT, M. A., J. C. AREZZO, AND H. G. VAUGHAN, JR. A laminar analysis of the cortical flash visual evoked potential in the monkey. *Soc. Neurosci. Abstr.* 9: 1194, 1983.
144. KRNJEVIĆ, K. Chemical nature of synaptic transmission in vertebrates. *Physiol. Rev.* 54: 418–540, 1974.
145. KRNJEVIĆ, K., M. RANDIĆ, AND D. W. STAUGHAN. Nature of a cortical inhibitory process. *J. Physiol. London* 184: 49–77, 1966.
146. KUFFLER, S. W. Discharge patterns and functional organization of mammalian retina. *J. Neurophysiol.* 16: 37–68, 1953.
147. KUHNT, U. Visuelle Reaktionspotentiale an Menschen und Katzen in Abhängigkeit von der Intensität. *Pfluegers Arch.* 298: 82–104, 1967.
148. KULIKOWSKI, J. J. Pattern and movement detection in man and rabbit: separation and comparison of occipital potentials. *Vision Res.* 18: 183–189, 1978.
149. KULIKOWSKI, J. J., P. O. BISHOP, AND H. KATO. Sustained and transient responses by cat striate cells to stationary flashing light and dark bars. *Brain Res.* 170: 362–367, 1979.
150. KUPERSTEIN, M., AND D. WHITTINGTON. A practical 24 channel microelectrode for neural recording in vivo. *IEEE Trans. Biomed. Eng.* 28: 288–293, 1981.
151. KURTZBERG, D., AND H. G. VAUGHAN, JR. Electrophysiologieal observations on the visuomotor system and visual neurosensorium. In: *Visual Evoked Potentials in Man: New Developments*, edited by J. E. Desmedt. Oxford, UK: Clarendon, 1977, p. 314–331.
152. KWAN, H. C., AND J. T. MURPHY. A basis for extracellular current density analysis in cerebellar cortex. *J. Neurophysiol.* 37: 170–180, 1974.
153. KWAN, H. C., AND J. T. MURPHY. Extracellular current density analysis of responses in cerebellar cortex to climbing fiber activation. *J. Neurophysiol.* 37: 333–345, 1974.
154. KWAN, H. C., AND J. T. MURPHY. Extracellular current density analysis of responses in cerebellar cortex to mossy fiber activation. *J. Neurophysiol.* 37: 947–953, 1974.
155. LANDAU, W. M. Analysis of electrical response to antidromic pyramidal tract stimulation in the cat. *Electroencephalogr. Clin. Neurophysiol.* 8: 445–456, 1956.
156. LANDAU, W. M. Evoked potentials. In: *The Neurosciences*, edited by G. L. Quarton, T. Melnechuck, and F. O. Schmitt. New York: Rockefeller Univ. Press, 1967, p. 469–482.
157. LANDAU, W. M., AND M. H. CLARE. A note on the char-